Environment CANADA Environnement
1020926I VOL ISS 65 850700
EXC # 001
TD 171.5.C3 R46
REPORT EE

OOFF

OIL SPILL REMOTE SENSING EQUIPMENT TEST PROTOCOL

OIL SPILL REMOTE SENSING EQUIPMENT TEST PROTOCOL

by

Moniteq Ltd.
Concord, Ontario

This report has not undergone detailed technical review by the Environmental Protection Service and the content does not necessarily reflect the views and policies of Environment Canada. Mention of trade names or commercial products does not constitute endorsement for use.

This unedited version is undergoing a limited distribution to transfer the information to people working in related studies. This distribution is not intended to signify publication and, if the report is referenced, the author should cite it as an unpublished report of the Branch indicated below.

Any comments concerning its content should be directed to:

Environmental Emergencies Technology Division
Technical Services Branch
Environmental Protection Programs Directorate
Environmental Protection Service
Environment Canada
Ottawa, Ontario
K1A 1C8

EE-65

July, 1985

1.0 INTRODUCTION 1
1.1 Purpose 1
1.2 General Overview Of This Study 1
1.3 The Interaction Of Oil With Electromagnetic Radiation 2
1.3.1 Ultraviolet 3
1.3.2 Visible 4
1.3.3 Near Infrared 4
1.3.4 Thermal Infrared 5
1.3.5 Microwave 5
2.0 DESCRIPTION OF THE CLASSES 6
2.1 Electro-optical Imaging Devices; Cameras 6
2.2 Electro-optical Imaging Devices; Scanners 8
2.3 Profiling Instruments 11
2.3.1 Radiometers 12
2.3.2 Gas Cell Correlation Spectrometer 13
2.4 Radars 15
2.5 Lasers 16
2.5.1 Types Of Oil And Their Spectra 16
3.0 CHARACTERIZING THE SENSORS 18
3.1 Signal-to-Noise Estimates 18
3.1.1 General Signal-to-Noise 19
3.1.2 Radar Signal-to-Noise 21
3.1.3 Fluorosensor Signal-to-Noise 22
3.1.4 Oilspils Signal-to-Noise 24
4.0 ENVIRONMENTAL PARAMETERS INFLUENCING THE SIGNAL . 24
4.1 Influence On The Physical Properties 24
4.2 Influence On The Radiometric Properties 25
4.3 Influence On The Overall Signal Quality 27
5.0 OPERATIONAL PARAMETERS INFLUENCING THE SIGNAL . . 29
5.1 Increased Surface Reflectance In The Near UV To Near IR 31
5.2 Change In Thermal Emissivity And/or Temperature 33
5.3 Change In Radar Backscatter 33
5.3.1 Altitude And Incident Angle Vs Radar Instantaneous FOV 35
5.3.1.1 IFOV Calculation For SCATTEROMETER Type Radar 36
5.3.1.2 Calculation For IFOV For SLAR 37
6.0 FALSE ALARMS 38
7.0 MINIMAL/MAXIMAL OIL DETECTABLE 39
7.1 Oilspils Sensor 39
7.2 Radars 40
7.3 Lasers; Fluorosensor 40
8.0 OPERATIONAL ABILITY 41
8.1 Electro-optical Imaging Devices; Cameras 42
8.2 Electro-optical Imaging Devices; Scanners . . . 44
8.3 Profiling Instruments 46
8.4 RADARS 48
8.5 Lasers 50
9.0 THE TEST PROTOCOL 52
10.0 DEMONSTRATION OF THE PROTOCOL 56
11.0 SUMMARY 56
12.0 REFERENCES 58

1.0 INTRODUCTION

1.1 Purpose

The rapid location and tracking of oilspills is becoming increasingly more important in Canada as offshore oil reserves are being tapped. Many passive and active remote sensors have been tested and proven effective for these purposes but to date no standard method for comparing the field performances of the different sensors has been established. In the field, sensor performance will be dominated by environmental and operational conditions and often these conditions may preclude the use of a particular sensor. The development of a test protocol that will provide field performance data that is meaningful to the average user is required.

1.2 General Overview Of This Study

This study attempts to prepare a test protocol by investigating the mathematical and physical relationships necessary to measure simple performance parameters for oilspill remote sensing devices. The performance parameters are:

- minimal oil detectable
  - by area
  - by thickness
  - by type
- maximal oil detectable
  - by area
  - by thickness
  - by type
- haze interference
- fog interference
- discrimination between thick and thin
- areal coverage
- daylight dependency
- sea state dependency

Because of the wide variety of sensors and detection schemes the development was divided into five parts where each applies to a particular class of sensor. The five classes are as follows:

- Electro-optical Imaging Devices, Cameras
- Electro-optical Imaging Devices, Scanners
- Profiling Instruments

- Radars
- Lasers

To be able to remotely detect oil at sea some physical difference between the oil and the background must be inferred by means of radiometric measurement. The physical properties of importance are the reflectance, emitance, transmittance and luninescence of oil with respect the surounding medium. The radiometric measurement of the upwelling and possibly the downwelling radiant flux is made and from that the physical property is deduced. This implies that not only the physical properties of oil in or on water and ice must be understood and modeled but also the ambient radiometric properties. Both environmental and operational conditions must be considered in the modeling.

The effect of the environment on the detectablity of oil will manifest itself in two ways. The first will be the interaction of the environment with the physical properties of the oil that are used to detect it. The second will be the degradation of the radiometric signal used to infer the physical property. The effect of operational conditions will be only to degrade the signal when using a passive sensor but when considering radars and lasers the production of the source signal will be affected by operational parameters. A block diagram of the basic structure of the protocols is shown in figure 0.

1.3 The Interaction Of Oil With Electromagnetic Radiation

To remotely sense oil at sea, an understanding of the how the various regions of the electromagnetic spectrum will interact with the oil is necessary. The detection of oil is based on the contrast between the oil and the background and will be due to the differences in the reflectivity, emissivity, transmissivity, luminescence, form, or texture. The contrast may be enhanced by an appropriate choice of measurement wavelength, period of observation, polarization, observation angle or other operational parameters. The contrast will be degraded by transmission of the electromagnetic signal through the atmosphere and by other atmospheric and oceanographic conditions. Each region of the spectrum will be affected differently and so the spectrum has been broken into the usual bands for further discussion.

FIGURE 0

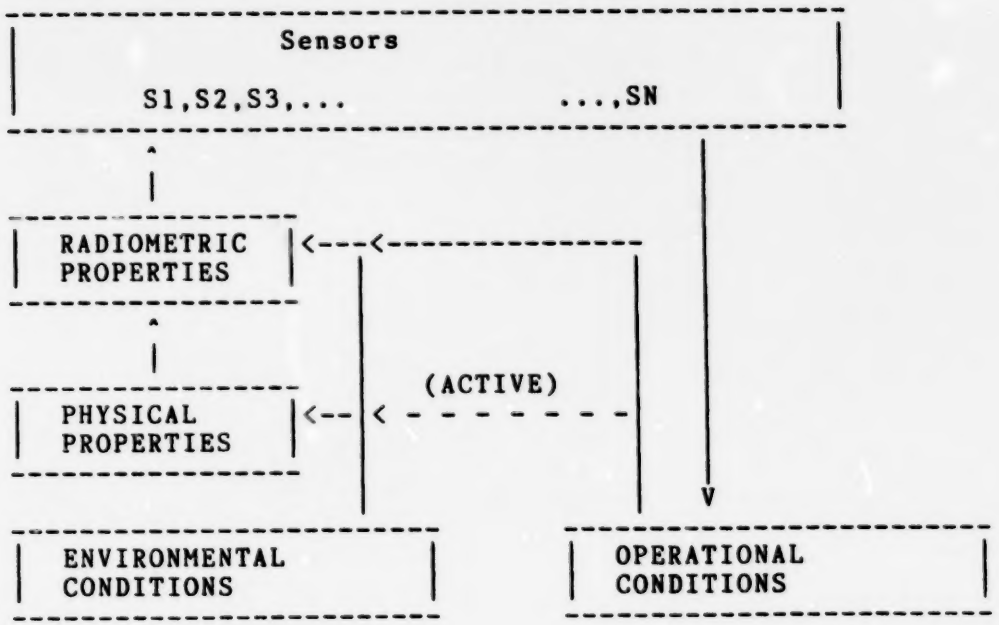
Sensors
S1,S2,S3,...
...,SN
RADIOMETRIC PROPERTIES
PHYSICAL PROPERTIES
(ACTIVE)
ENVIRONMENTAL CONDITIONS
OPERATIONAL CONDITIONS

1.3.1 Ultraviolet -

In general, ultraviolet radiation (UV) is significantly more reflective when incident on oil than on water. The increase in the measured radiance will be due to the large surface reflected component which is strongly polarized. At the same time oil is a strong absorber of ultraviolet radiation. When the oil slick is thick (> 10 μm) the attenuation of the radiance upwelling from below the oil slick (the volume reflected component) can be large enough that the increased surface reflectance is counterbalanced. When viewed at or near the Brewster angle the surface component will be stongly horizontally polarized and the volume component will be slightly vertically polarized, so the two signal components can be seperated by linear polarizers.

The far ultraviolet (0.2 - 0.3 μm) is severely attenuated by the atmosphere and so is useless for detecting oil. The useful ultraviolet region extends from 0.3 to 0.4 μm.

1.3.2 Visible -

The visible spectrum (Vis) must be further broken down to describe its utility for oil detection. The violet region (< 0.4 μm) was considered in the previous section under ultraviolet. Between 0.45 and 0.5 μm the reflectivity of oil is nearly identical to that of water and so direct detection by reflectance contrast is impractical. In the spectral region greater than 0.6 μm the reflectivity is again higher than for water. Any band in the visible region can be used for oblique angle detection of an oil slick. When viewing in the sun's glitter pattern any slick will appear as a sharply contrasting dark feature. Oil detection using the visible spectrum is quite limited.

1.3.3 Near Infrared -

The reflectance of oil in the spectral region 0.7 to 1.2 μm (NIR) is 20 to 100% higher than for water under daylight illumination and up to 50% higher under only starlight and airglow illumination. The volume reflected component of the NIR signal is always small so the slick

thickness does not adversely affect detectablity as in the UV.

1.3.4 Thermal Infrared -

The thermal infrared (TIR) is one of the most useful and one of the most complex spectral regions when used for oil detection. The contrast in the signal between oil and water will depend on the emissivity, surface temperatures, thermal conductivity, thermal diffusivity, solar heating and evaporation rates. Generally oil has a lower emissivity than water and so will appear cooler but the physical temperature of the oil may be quite different from the water. For example, the oil may absorb solar energy for an increased temperature or the volitile components may cool the oil by increased evaporation. Some form of temperature distribution will inevitability occur that will distinguish the oil from the water since it is very unlikely that all the variables will just balance rendering the oil undetectable. Because of absorption only the atmospheric windows 3.0 to 5.0 μm and 8.0 to 14.0 μm are normally used.

1.3.5 Microwave -

Microwave radiation can penatrate cloud, fog, some rain and can be used both day and night. The spectrum extends from 1 mm to 1 m but radiometers should be operated at wavelengths less than 8 mm. The emissivity of oil is greater than that of water and so a thick film on calm seas will appear brighter. The calming effect of a oil on rougher sea can lower the surface temperature within a slick and oil will appear as a lower brightness temperature. Generally, the detectablity of oil will improve as the wavelength is shortened down to a limit determined by the surface capillary wavelength. When radars are used the dampening of the capillary waves reduces the backscatter (when the appropriate look angle is used) and the slick appears as a dark feature superimposed on a bright background.

2.0 DESCRIPTION OF THE CLASSES

2.1 Electro-optical Imaging Devices; Cameras

Electroptical Imaging Cameras, commonly called Television Cameras, are non-scanning imaging systems that can be used in the UV through TIR spectral regicns. The scene of interest is optically focussed onto a photoconductive or photoemissive surface on the evacuated image tube. A readout electron beam is electromagnetically or electrostatically deflected to scan the photosensitive surface. The output is in a raster format that can be displayed on a television monitor in real-time or stored on magnetic tape.

The spectral range is approximately 0.12 to 1.8 μm but is dependent on the type of tube and with detector cooling can be extended to 14.0 μm. Often spectal bandpass filters are used to improve the contrast between the oil and the background signals. The sensitivity and the dynamic range of the tube may be fixed for a particular illumination level or may be adjustable. Auto irising permits the tube's use in bright sunlight through to low light levels. Image smearing is caused by a lag in the response time of the image tube that indicates either high signal levels or poor tube quality. Smearing can cause a target to be missed. Image tubes are characterized by the slope (gamma) of their transfer curve. A high gamma indicates high sensitivity and low dynamic range and low gamma large dynamic range and low sensitivity. A compromise intemediate gamma is normally required for oil detection.

The conventional vidicon camera is an important type of television sensing tube. The vidicon is a cylindrical glass envelope containing an electron gun at one end and a target and faceplate at the other. The tube is surrounded by a yoke containing electromagnetic focus and deflection coils. The faceplate is coated on the inside with a thin layer of photoconductor over a thin transparent metal film that forms the target. Behind the target is a postively charged fine wire mesh. Electrons are decelerated after passing through the mesh and reach the target with apporximately zero velocity. A small positive charge is applied to the metal coating of the target. In darkness, the photoconductor behaves as a dielectric, and the electron beam deposits a layer of electrons on the inner surface of the photoconductor to balance the positve charge on the metal coating. Thus, after a complete scan by the electron beam, the photoconductor appears as a capacitor with a positively

charged plate on one side and a surface charge of electrons on the other.

When light strikes a small area of the photoconductor, it allows the electrons to flow through, locally depleting the electron charge layer. Thus, if an optical image is formed on the target, the photoconductor will form an identical electron image on the back of the target, That is, electrons will be present in the dark areas and absent in the light areas. As the electron beam scans the target, it replaces the lost electrons, restoring the uniform surface charge. As the electrons are replaced, a current flows in the external target circuit. This current is proportional to the number of electrons required to restore the charge and, therefore, to the light intensity at that point. It is also proportional to the beam velocity, which, in turn, determines the time available for the charge to flow. Current variations in the target circuit produce the video signal of the vidicon. The electron beam repeatedly scans the surface of the target, replacing the charge that bleeds away during the interval between scans. the vidicon target is thus an integrating sensor.

Some modifications have been made to the conventional vidicon camera that have resulted in the Return Beam Vidicon, Plumbicon, silicon diode array and silicon intensifier camera tubes.

The return-beam vidicon (RBV) camera differs slightly from the conventional vidicon camera in the mechanism used for scanning the image. A weak electron beam is reflected from the photoconductive surface, and the video signal is produced by the modulation in the reflected beam created by depletion as the beam passes over positively charged regions. Amplification of the signal is done by a cascade of dynodes. The charge pattern is erased by discharging the photoconductor which is then prepared for the next exposure by scanning with a relatively high current beam. The advantages of the RBV over the conventional vidicon are higher gain factors and higher spatial resolution.

The photoconductive target of the standard vidicon is made of selenium photoconductor. A similar tube, the plumbicon, has a lead oxide target. This tube is somewhat more sensitive than than the vidicon and is applicable to low-light-level situations.

More recently, the silicon diode vidicon was developed which uses a silicon photoconductor target doped with N-type impurities. An array of small P-type islands is diffused into the silicon target. This produces a rectangular array of dicrete silicon diodes for the photosensitive surface, from which the video signal is extracted.

The Silicon Intensified Target (SIT) camera tube consists of a silicon target vidicon coupled with an image intensifier. The image intensifier acts as a preamplifier to the television tube which uses a silicon target. The SIT is particularly well suited to low-light-level applications because of its high sensitivity and low blooming, as well as good picture quality.

Examples of these sensors with their operating ranges are listed below.

RCA Low-Light-Level Television

The LLLTV is a SIT television camera, usually outfitted with UV and NIR transmission filters and Polaroid HNP'B polarizing filter. Images are viewed in real time or recorded on magnetic tape.

Pyro-Electric Vidicon

A thermal imager that operates in the IR atmospheric windows to produce real-time imagery or video tape.

2.2 Electro-optical Imaging Devices; Scanners

Passive electro-optical remote sensors are used to measure the energy reflected or emitted by a target medium, which is illuminated by some natural source such as sunlight and skylight. Although the source spectra is continuous (ie. like sunlight), the detector is designed to record only select spectral bands. These bands are determined by the configuration of the sensor, and the spectral filtering techniques used.

These sensors are typically classified into two groups, imaging, and non-imaging. A nonimaging device, like a radiometer provides spectral intensity information over a number of bandpasses but contains no information with respect to the geometry of the scene being sampled. A multispectral imager, however, is capable of scanning a

scene to build up a two dimensional "picture"; one picture for each wavelength measured. The data from these devices may be stored on various media, ranging from photographic film, to computer compatible tape, the latter being the most practical and common when post flight analysis is required.

The nonimaging sensors may be mounted on any moving or stationary platform as required by the operatoring conditions. Imagers are designed with optics that scan in one dimension only (ie. across track), and thus they are mounted on moving airborne vehicles (ie. aircraft, satellite) since they depend upon forward motion to build up the second (ie. along track) dimension of the "picture". A number of reliable commercially available imagers are now available, which use various scanning and electro-optical technologies.

Passive line scanner devices are capable of observing a scene in two dimensions, to recreate the geometry of the target being studied. In reality this geometry is distorted as a result of the aircrafts attitude variations from outside influences such as cross winds etc. Scanning is performed by mechanical or electronic means in one dimension, such that the imager scans from side to side as an aircraft moves over the ground. The individual picture elements, or "pixels", which a digital scanner would acquire, are individual IFOV's of the ground.

Mechanically scanned systems use a front surfaced mirror/prism on a shaft that is oriented parellel to the flight line. The across track motion of the spinning mirror/prism, and the along track motion of the aircraft, produces a continuous raster of swaths to build up an image of the scene below.

In the pushbroom scanner, the across track scene is projected onto a diode array, and the vehicles forward velocity causes the image path to build up in the other dimension. The array is repeatedly sampled to build up the scan lines of the image. The detector array is sampled at the appropriate rate to produce contiguous lines. All mechanical disturbances are removed in this type of system, since the scanning is done electronically. In addition, very accurate band-to-band registration and accurate mapping of terrain is possible. Greater S/N is realized as a result of the large area of the focal plane from which the signal is continuous gathered. This improved sensitivity increases the radiometric accuracy and allows for narrower bandwidths. This technology is relatively new and the operation of this

type of scanner is presently restricted to visible and near infrared portion of the spectrum.

The detector system is usually a solid state device, but may also be a photoelectric tube which contains indium antimonide or a similiar compound. Most detectors must be kept at low temperatures to minimize detector noise, and improve the S/N ratio, especially in the thermal IR region.

After amplification, the digital signal is usually viewed inflight on a realtime display, and simultaneously recorded on high density digital tape. It may also be recorded on 70 mm film.

Multispectral (MSS) imagers are different from thermal scanners, or radiometers because they are capable of imaging in different bandpasses simultaneously, this provides greater interpretative capability for signature analysis. The MSS mechanicals are similiar to those of other scanners, but with the addition of a light dispersion assembly such as a prism or diffraction grating. Individual detectors (or CCD, CID arrays) are geometrically placed within the dispersed light beam to sense the energy in each band of interest. An image is produced for each channel, and by assigning a colour to each channel and superimposing them on a colour video display, a composite colour image of the scene is recreated.

Thermal IR and MSS imagery have been used in ice measurements, geological mapping, oceanographic surveillance, depth mapping, water quality mapping, and oil spill detection/monitoring by both satellite, and airborne platforms. However, these scanners have some disadvantages and advantages when compared with photogaphic systems.

The advantages include:

- Measurements can be made in the visible, UV and IR spectrum.
- Narrower bandpasses are possible.
- The output may be displayed in realtime, or stored on computer compatible tape for later more detailed analysis.
- Wider dynamic range and sensitivity.
- Data is easily calibrated.
- Thermal imagers can operate by day or night.

The disadvantages include:

- Lower spatial resolution.
- Systems are larger.
- System are more expensive.
- Scanner images are susceptible to aircraft high frequency attitude variations.
- The lateral scale of the scanned image can change across the flight line.
- The radiance levels in thermal imagery can change along a flight line due to variations in the intervening atmosphere.

An example of the sensors with their operating ranges listed below with any modifications or filters applied as suggested in the above discussion.

CCRS Multispectral Scanner (MSS)

The MSS is an imager with up to ten channels are chosen between (.38-12.1 μm). The scanner has as 85.9 deg FOV with a spatial resolution of 2.5 mrad.

CCRS Dual Channel Line Scanner (DCLS)

The UV channel covers from .27-.37 μm, with a swath width of 77.3 deg and a resolution of 2.5 mrad.

CCRS Multi-Element Imaging Sensor (MEIS)

MEIS is an imager which uses one-dimensional CCD array technology. It presently contains five operational cameras. Spectral bands are defined using filters over the entrance apature of each camera.

MONITEQ Programmable Multispectral Imager (PMI)

Formerly the FLI the PMI is a band programmable imager using two-dimensional CCD array technology. It selects up to 8 channels from 288 spectral channels at a resolution of 2.6 μm, over the range .430-.800 μm.

2.3 Profiling Instruments

These instruments utilize electronic energy detectors and are designed to sense energy in a number of narrow spectral band simultaneously and display emittance (or reflectance) spectrum of oil slicks. The profiling instrument is a passive electro-optical remote sensor, and

is able to detect oilspills by sensing the spectral radiation (reflected or emitted) from the oil itself or from the evaporated gases above the oil.

2.3.1 Radiometers -

Absolute and relative radiation levels may be measured by a radiometer. For absolute measurements, a known reference source is used to calibrate the instrument. The detector itself (DC radiometer), or a radiation chopping system (AC radiometer) can be used to measure the reference source. The AC chopper-mirror system is the most common, it alternately measures the incoming radiation and the reference radiation. The reference sources for IR instruments are typically temperature controlled backbodies.

Infrared radiometers operating from about 0.75 μm are normally designed to measure the thermal emission form the target. Daytime sytems are confined to the atmospheric windows from 4.5-5.5 μm and 8.5-13.5 μm, and nighttime operation is restricted to the longer wavelengths around 8.5-13.5 μm. IR systems do not work when fog or cloud cover intervenes.

The materials used to detect IR or UV energy differ. Photon energy is inversely proportional to wavelength. In the higher energy end of the spectrum (ie. UV), photoemissive detectors are used, since the energies received are sufficient to free electrons from the photoreactive material. Beyond 1.0 μm, the photon energy are too low to use this type of detector, and thus photoconductive, photovoltaic, or photomagnetic materials are used.

Detector sensitivity depends upon the temperature of the reference signal, the bandwidth, detector receiving area, wavelength to be detected, and the signal chopping frequency.

The energy collection sytem for radiometers varies with their application. Directional capability is required for aiming the sensor at distant targets, and the optical train will be constructed from different materials depending upon the wavelengths of interest. For example, lens are used in the visible, and near IR regions, whereas mirrors typically used for thermal radiation. For a multi-wavelength radiometer, a mirror system, will work equally well for UV,

visible, and IR radiation, although the detectors will be quite different.

Common solid state detectors are photoresistors, and photodiodes. They are sensitive to different spectral regions depending upon the materials they are made from, and those operating in the thermal bands are often cooled externally to reduce thermal noise and increase sensitivity. To detect energy within a specific bandpass, a filter or dispersion system such as a prism or diffraction grating is used, by placing the detector in the proper geometric position to recieve the spectral range of interest. Obviously, no filtering is required if one wishes to measure the total incoming flux.

2.3.2 Gas Cell Correlation Spectrometer -

In this type of the sensor the amount of target gas present with a particular spectral band structure is measured by the difference in signal resulting when the incoming light is passed alternately through a spectrally neutral filter and a matched filter achieved with a sample cell of the gas to be sensed. The signal passing through those two cells is precisely measured, and subsequently balanced electronically to be the same when no gas is in the sensor line of sight. This balance condition is then upset by the presence of gas spectral absorption or emission in the incoming light. Further discussion is based on the Oilspils sensor built by Moniteq Ltd.

The basis of operation of the sensor is the differential transmission, through separate reference and measurement gas cells, of radiation entering the sensor. The limiting constraint on sensor performance is the temperature contrast between the water and air. This is evident in the defining expression for the oilspills (difference) signal;

$$S = N_c A(eB_e - B_a)(\overline{T_a T_c} - \overline{T_a}\,\overline{T_c})\Delta\omega + J_c$$

where

S - difference in transmitted energies betweer correlation gas cell and the reference cel

N_c - transmission coefficient of the optical components for correlation channel

e - emissivity of the earth's surface

A - optical throughput of the optics

B - blackbody radiance at frequency and temperature theta

T - Transmission

J_c - emission term from the correlation gas

subscripts a, c and e designate the atmosphere, correlation cell and earth respectively.

The term (TaTc - TaTc) is termed the correlation coefficient. Once the instrument is calibrated the difference can be represented approximately by

$$S \simeq C \Delta T F$$

where C is a constant which depends on system parameters and F is a path length in ppm-m, and ΔT is the temperature contrast between the ground and air.

This sensor is most sensitive in conditions where a large temperature contrast exists (ie. clear,cloudless days with minimum wind speed). In principle the sensor could operate at night but the lack of good temperature contrast due to air/surface thermal equilibrium usually results in poor S/N characteristics. Since Oilspils makes a measurement of the gas which evolves from the oil spill it does not provide a measure of the thickness of the oil layer. However, it can distinguish between oil and background since it correlates with the spectra of the oil layer gaseous by-products.

Examples of these profiling sensors with their method of operation is given:

MONITEQ OILSPILS

A gas cell correlation spectrometer that operates by detecting the trace gases evolved from the oil layer.

CCRS Miller-Pieau Photometer (MPPH)

A four channel profiling radiometer with a downwelling detector. Spectral bands are chosen by filtering in the near visible spectral region.

CCRS Optical Multi-channel Analyzer (OMA)

The OMA is a 500 spectral channel spectrometer capable of resolving 0.1 nm. Both upwelling and downwelling spectra are measured.

2.4 Radars

The radar system operates by transmitting energy in the microwave spectrum and mapping the energy reflected from physical surfaces lying in the beam path. It is the backscattering property of the target surface which determines the strength of the signal diffusively reflected or scattered back to the receiving antenna.

Therefore, radars present a measure of the targets' back-scattering property relative to an adjacent target area, providing an image of the ocean surface.

Radars ability to detect oil spills is based on the effect which oil film has on the backscattering intensity of the target area. Basically, even a very thin oil film on the water's surface suppresses the formation of capillary waves and gravity waves of up to 10 m in length. It is the presence of the capillary waves which increases the back-scattering intensity recieved by the radar system. The suppression of capillary waves by the oil film calms the water thereby producing a 'slick'. This in turn reduces the backscattering intensity recieved by the radar system. The formation of capillary waves is caused mainly by sea surface winds and is discussed in more detail later.

Slicks can be caused by other phenomena such as internal waves, freshwater "streams" lying on seawater surface, frazil or grease ice and ships wake to mention a few. These other causes of slicks which can give rise to false detection of oil slicks may limit the use of radar in certain environmental conditions. Therefore, it is desirable to have an open sea.

The advantages of radar systems is its ability to cover large areas, operate in moderately adverse weather conditions and is daylight independent. But the only information radars provide is the magnitude of area of the oil slick. Other information such as thickness and type of oil cannot be provided by radars.

Examples of radars are:

CCRS Scatterometer

Active profiling sensor operating at 13.3 GHz (2.25 cm). Both H & V transmit and receive. Data recorded on magnetic tape.

ERIM Synthetic Aperature Radar (SAR)

Active imaging sensor operating in X,L bands. H & V transmit and receive. Adjustable depression angle. Data recorded on magnetic tape or film.

2.5 Lasers

Lasers are used to stimulate fluorescence in the oil which can be positively identified by correlation with known spectra. In this technique an airborne laser illuminates a small area on the water surface. Any fluorescence signal induced by laser light is monitored through a telescope by an optical receiver also situated in the aircraft. If a pollutant has fluorescence properties different from the background, it can be detected and characterized. The oil fluorescence spectra can be distinguished from sea water background, and, it has been shown by laboratory studies, that it can be classified into light refined, crude and heavy refined oils [1,2,3,14]. The fluorescence emission is analyzed by a spectrometer in the receiver and is displayed as a 16 channel spectrum (intensity as a function of wavelength).

2.5.1 Types Of Oil And Their Spectra -

Since the Fluorosensor can correlate the detected spectra with a table of known spectra and so positively identify the type of oil, it is appropriate to discuss the types of known oil spectra and the distinctions that may be

made.

1. Light oil refined

   a. Strongly partly structured emission spectrum

   b. Peak wave length max = 400nm

   c. Decay time > 10 ns

Different light oils cannot be distinguished from each other.

2. Crude oil

   a. Broad unstructured emission spectrum

   b. Peak wavelength max (400-500) nm
      intensity (.5 to 1 times of the light oil)

   c. Decay time < 2 ns

Different types of oil within the class cannot be identified.

3. Heavy refined oil

   a. Very broad unstructured emission spectrum

   b. max > 530 nm

   c. Decay time < 2 ns

Individual oil in this group cannot be distinguished.

An example of a laser Fluorosensor is given:

CCRS MK III Laser Fluorosensor

A pulsed UV laser with an active range gated fluorescence detector. Measured spectra correlated with known oil spectra by type.

3.0 CHARACTERIZING THE SENSORS

The characteristics of a detector can be described by the following:

* Spectral Response
* Speed of Response
* Signal-to-noise

All of these characterisitics will be important in determining if a particular detector will be appropriate for detecting oil at sea. The spectral response will determine if the sensor is operating in the correct spectral region for detecting a contrast between oil and the background signal. The speed of response will determine the temporal resolution of the sensor and limit the spatial resolution. The signal-to-noise ratio will ultimately determine the quality of the signal from which the inference of the presence of oil must be made. The spectral and speed response of a sensor are essentially dictated by the design and are generally unaffected by environmental conditions prevalent at the sea surface.

It is the estimation of the signal-to-noise ratio (S/N) of the complete system which will be the basis of the test protocol derived herein. This was judged to be the most fundamental quantity which could be determined for each sensor under ideal operating conditions and which could then be degraded according to the prevailing atmospheric, oceanographic and operational conditions to arrive a consistent measure of sensor performance.

3.1 Signal-to-Noise Estimates

Estimation of the signal to noise ratio will depend on what signal is being measured and the type of detector used. A general discussion of the S/N is possible for electro-optical imaging cameras, scanners and radiometers. More specific discussion is required for radars, lasers and gas cell correlation spectrometers.

3.1.1 General Signal-to-Noise -

The two basic types of detectors are quantum detectors and thermal detectors. In a quantum detector photons interact directly with the elctronic energy levels to produce free charge carriers. A thermal detector is heated by the absorption of radiant flux incident upon it and this indirecty affects its electrical properties.

Quantum detectors can be divided into two groups photoemissive and solid-state detectors. Solid-state detectors can be further subdivided into photoconductive and photovoltaic devices. Slater (1980) gives the S/N for photoemissive, photoconductive and photodiode type detectors.

For a photoemissive detector (for example photomultiplier tubes PMT) the spectral S/N is given by

$$S/N = MTF\, a^2 D \left| \frac{K\, k_s\, n}{4\, k_f\, (v/h)\, \theta\, k_\sigma\, e} \right|^{1/2}$$

$$\times \left| \int_{\lambda 1}^{\lambda 2} E_{1\lambda} \frac{\Delta_p(\lambda)}{p_B(\lambda)} R(\lambda)\, t_u(\lambda)\, t_o(\lambda)\, d\lambda \right|^{1/2}$$

where

MTF	-	Modulation transfer function of the total optical system
a	-	IFOV
D	-	diameter of the entrance pupil
K	-	constant dependent on detector area and IFOV
k_s	-	scanning efficiency factor
n	-	number of detectors in parallel in each channel
k_f	-	ratio of the filter effective noise bandwidth to the information bandwidth
v/h	-	velocity-to-altitude ratio

θ - angular cross track width
k_σ - detector noise multiplication factor
e - electron charge
E_λ - spectral irradiance
R - spectral responsivity of the detector
p_B - reflectance of background
ΔP - reflectance difference between the background and the feature
t_o - transmittance of the optical system
t_u - transmittance of the atmosphere

For a photodiode detector (for example the silicon diode linear array) the spectral S/N is given by

$$S/N = \frac{K \, MTF \, a \, D^{3/2}}{4 \, i_n} \left| \frac{2 \, k_s \, n}{k \, (v/h) \, \theta_f} \right|^{1/2} \times \int_{\lambda 1}^{\lambda 2} E_{\lambda 1} \, \Delta p(\lambda) \, R(\lambda) \, t_u(\lambda) \, t_o(\lambda) \, d\lambda$$

where

i_n - total AC noise current

And finally for the photoconductive detector the (for example the conventional vidicon) the S/N is given by

$$S/N = \frac{\pi K\, a\, D\, MTF}{4n\, N_f} \left| \frac{2\, k\, n_s}{k\,(v/h)\,\theta} \right|^{1/2} \times \int_{\lambda_1}^{\lambda_2} \Delta L_\lambda\, D^*(\lambda, f_0, \Delta f)\, t_u(\lambda)\, t_o(\lambda)\, d\lambda$$

where

$D^*(\lambda, f_0, \Delta f)$ - spectral detectivity
ΔL_λ - spectral radiance
n_f - electronics noise

3.1.2 Radar Signal-to-Noise -

The interaction between electromagnetic radiation emitted by the radar system and atmospheric conditions such as haze, cloud, fog and precipitation serve to attenuate the signal strength. It is the absorption of the water droplets which the signal passes through which causes the attenuation. To determine the theoretical loss due to absorption caused by water droplets, the empirical model of Goldstein (1951) and Staelin (1966) based on properties of Standard Cloud Models[2], the following formula

$$Y = (m*10^{**}(0.0122(291-T)-6))/\lambda^2 \text{ [nepers/cm]}$$

where m = mass density of medium [g/m**3]
T = temperature of medium [K]
λ = (free space) wavelength of incident radiation. Note: $\lambda = c/f$
(f=radar operating frequency,
c=speed of light = 3x10**3 m/s)

yields the loss per cm of distance travelling through

medium. In order to correlate with the same units as backscatter which is in power units of decibels dB, the following resultant equation yields the attenuation loss

$$La = Y \times 8.68 \times 10^{5} \times Lpath \quad [dB]$$

where Lpath = distance which signal must pass through medium.

Since the detection of oil slicks is the relative difference between backscatter intensity of an area with and without the oil slick then the attenuation of both signals does not effect the detection of oil. Therefore, the advantage of a radar in moderate climatic conditions. The limitation is when the attenuation reduces the signal to within 6 dB of minimum detectable signal. At this point the probability of detecting of oil slicks is very poor and such a scenario is encountered when heavy rain or snow exists.

The above model represents a first order approximation whereby the Rayleigh limits are satisfied. The above model does not consider scattering effects which may be dominant at the higher operating frequencies. Also, the model indicates a higher attenuation with higher operating frequencies ($\lambda = c/f$) whereby

$$La \sim 1/\lambda^{2}$$

3.1.3 Fluorosensor Signal-to-Noise -

The signal in photon counts for a lidar fluorosensor is given by (ref. [9])

$$S = (\lambda_{ex}/hc) EO \cdot Tl \cdot Tf \cdot Ts \cdot Tr \cdot C(\lambda)\, d(\lambda)\, Ar\, n(\lambda)$$

$$\times (1 - \exp[-a_{ex} D]\,)/(4\pi H^{2}) \qquad \text{(photons)}$$

where the parameters are defined in the ref. [9] report. For our purposes we can assign the values given in ref. [9] to those parameters which do not change considerably from one system to the next. This includes those transmission/ reflection effects which might be affected by sea state

since Raynor (ref. [10]) has shown that the spectral return is not significantly affected for the range of sea states expected in deep water. This yields;

$$S = (2.717 \times 10^{19}) EO \cdot \lambda \cdot Ta\ n(\lambda_{ex})$$

$$\times (1 - \exp[-a_{ex} D])/H^2 \qquad \text{(photons)}$$

where EO is the pulse energy in Joules, λ is channel wavelength (λ_{ex} is the excitation wavelength), Ta is the atmospheric transmission = exp(-2*tau(H)) and tau(H) is the optical depth from the surface to the sensor level, n(λ) is fluorescence conversion [nm**-1], aex is the total volume attenuation coefficient in oil at the excitation wavelength [um**-1] (assumed >> than a at the channel wavelength), D is the oil thickness in um, and H is the altitude. The fundamental indicator of performance for the fluorosensor is clearly the signal to noise ratio which assuming Gaussian statistics is given by;

$$S/N = S/[S + B]^{1/2}$$

where B is the received signal due to background radiation. This latter term is given by;

$$B = (\lambda/hc) I(\lambda) C(\lambda) d(\lambda) (At/H^2) Ar \cdot Tr \cdot t \qquad \text{(photons)}$$

For the fluorosensor receiver parameters given in ref. [9] (including a gate width of t = 50 ns) and typical upwelling radiance values (I(lambda) this term is negligible with respect to S. Thus the signal to noise is simply

$$S/N = S^{1/2}$$

3.1.4 Oilspils Signal-to-Noise -

According to recent calibrations performed by Moniteq Ltd. the abundance (PPM-Meters) of propane as a function of the Oilspills signal to noise (S/N) is given approximately by;

$$F = 130 * (S/N) / \Delta T \quad \text{ppm-m}$$

where ΔT is the temperature difference between the target gas and the background source. Propane is a characteristic evaporative product of oil.

For a minimum S/N of say 3 the minimum detectable abundance is

$$F_{min} = 400/\Delta T \quad \text{ppm-m}$$

4.0 ENVIRONMENTAL PARAMETERS INFLUENCING THE SIGNAL

The signal received by a remote sensor is influenced not only by the intervening media (atmosphere, haze, water) but also the background signal from the target area (ie. water, ice). The material properties of oil and water (or ice) create a measurable contrast difference in certain spectral bands, and this contrast difference is influenced by various parameters such as the target emissivity, reflectivity, energy polarization, observation angle etc. It is important to know these various contributions to the signal in order to quantify a series of measurements, so that a standard set of conditions may be used to predict the presents of the target, in this case oil.

4.1 Influence On The Physical Properties

Other influences on the signal involve measuring parameters not directly coupled with the radiative transfer of the reflected light. These include atmospheric, and oceanographic conditions such as weather patterns influencing sea state. In addition the aircraft is restricted to specific "weather windows", and the particular sensor used will also be confined to certain operating conditions such as daylight only, or low precipitation,

depending on its configuration.The physical properties of interest are the reflectance in the near visible spectral region the emittance in the TIR region and the suppression of capillary waves detected by backscatter in the microwave region.

The relationship between wind speed versus backscatter intensity can be defined by three wind velocity regions. From 0-2 m/s the formation of capillary waves by wind is negligible and would prove difficult for detection of oil slicks. The second region from 2-7 m/s generates a range from weakly developed capillary waves to strongly developed capillary waves. For 7-25 m/s is the optimum in terms of capillary wave generation which gives a maximum in backscatter signal strentgh. Therefore, the optimum condition for detecting oil slicks would be in the 7-25 m/s. The regions are defined by gathered flight data [14].

4.2 Influence On The Radiometric Properties

During the daytime it is clear that the spectral content of the sky and sun, influence the ablity of the passive sensors in detecting the oil slick. A clear sky has a high blue content, and polarization properties which favour directing the sensor away from the sun to minimize sunglint effects (Millard, 1971). This sky condition is good for detectors operating in the blue and UV regions since it offers higher signal levels. A flatter spectrum occurs during an overcast day, with a higher relative red component. Thus sensors optimized for the near-red end of the spectrum will benefit from higher signal levels.

At night, visible light imager cannot be used, however, IR scanners can be. The water is typically warmer than the ambient air and surrounding land mass at night, but the emissivity does depend on viewing angle. At near perpendicular angles, the emissivity of the water can be high (>0.8) giving a positive contrast, but at much lower angles the reflectivity increases, and thus the emissivity decreases giving a negative contrust. Sea state also effects the relative emissivity, for example, at at low grazing angles, the higher water turbulence increases the emissivity. Cloudy conditions tend to decrease the apparent temperature differences because of a reduced net heat loss due to a lower radiation flux coming from the cloud cover.

Detection of oil slicks over water bodies by infrared sensors depending on either a real temperture difference between the oil and water or an emittance differential. The change in radiance over the oil slick relative to water can be written

$$\Delta N(\lambda) = B(\lambda)dE(\lambda) + E(\lambda)dB(\lambda)$$

where $B(\lambda)$ is the black body expression

$$B(\lambda) = (2c^2 h/\lambda^5)(1/(\mathrm{Exp}(X)-1))$$

and

$$dB(\lambda) = B(\lambda)\ X\ dT/T$$

$$X = hc/\lambda kT$$

An appropriate measure of confidence in the contrast measurement is $\Delta N(\lambda)/dN(\lambda)$ where $dN(\lambda)$ is the instrumental radiance noise corresponding to thwe noise equivalent temperature dT.

Given

$$dB(\lambda) = B(\lambda)\ X\ dT/T$$

one can easily show that

$$S/N = \Delta N(1)/dN(1)$$

$$= (\Delta T(E) + \Delta T)/dT$$

where

$$\Delta T(E) = T\ dE(\lambda)/\ X$$

represents the apparent change in temperature due to an emittance differential. Note that the signal to noise can be minimal for a temperature rise which is equal and opposite to an apparent emittance related temperature drop.

If a temperature equilibrium exists (most likely during nightime or overcast conditions) then T(E) will dominate with $dE(\lambda)$ varying between 0 and -.05 depending on oil thickness (or T(E) will be between 0 and 3 K for 10.5 μm wavelength and temperature ~ 293 K; ref [17]). In sunlit

conditions thick oil layers can produce a real temperature increase, over an oil layer, as high as 10 K.

A typical value of dT is .04 C° (MSS Deadalus line scanner; 8.5-12.5 μm spectral range). Hence the ABS(S/N) value described above could be expanded to vary from unity to 3/.04 = 75 for temperature equilibrium condition and up to a maximum ~ 250 in sunlit conditions.

Temperature and emittance variations are however, no guarantee of positive oil identification. Variations in oil radiance are sufficiently large to preclude any identification/classification applications without supplementary measurements.

4.3 Influence On The Overall Signal Quality

Ultra-violet

Severe atmospheric attenuation prevents the detection of signal levels below 0.29 μm for the detection of oil on water. Oil has a significantly higher reflectance that water in the 0.3 to 0.4 μm region, and thus sensors operating in here have good potential to detect oil on water (Catoe and McLean, 1979).

Visible

The signal levels received in the visible spectrum, may be broken down into two components, the specular, and the diffuse. The specular component of the oil reflected light is always greater than that of the water, but the diffuse component is usually less. The maximum contrast between oil and water occurs in the ultraviolet-blue (<0.4 μm) region and the red (>0.6 μm) region. Minimal contrast is noted to occur between 0.45 and 0.5 μm (Catoe and McLean, 1979). It is clear then that sky conditions have a strong influence upon the ability to differentiate oil and water. Studies have shown that the best contrast is observed with an overcast sky.

Near IR

It has been noted (Catow and McLean, 1979) that in the near infrared, the radiance from an oilslick is higher than the background water by 20% to 100%. This spectral region is therefore very good for daytime oilspill detection. The

authors also state that there exists adequate diffuse illumination (from starlight and airglow) at night to allow approximately 50% greater radiance from oil compared with water. It is suspected that this observation was made with some sort of light intensification device, since no details were provided.

Mid and Far Infrared

In the Mid and Far IR, the termperature of the oil and water surface, thermal conductivity, evaporation rates, solar heating etc. are the major contributors to the signal levels. For example, at 8.5-12.5 μm the emissivity of the water is about 0.988 and oil is 0.94-0.97, thus the oil will have a radiant temperature lower than the water. The oil will appear cooler depending on its thickness and type, and can appear as much as 3 K lower.

An oil layer on the water surface can have a number of effects on the actual temperature of the surface (Neville, et al, 1979) as follows:

> "Optical thick oil can absorb sufficient solar irradiation to heat it above the water surface temperature."
>
> "Oil near the source of the spill may retain the source temperature which could be different from the water."
>
> "Volatile components from freshly spilled oil may provide cooling by increased evaporation."
>
> "Less volatile oils may impede evaporation of the water thereby producing a warming effect."
>
> "An oil film can impede the flow of heat at the water surface, resulting in an increased or decreased surface temperature depending on whether the air temperature is above or below the water temperature."

Microwave

In Figure 1 and Figure 2 are first order approximation of the influence on signal quality due to attenuation and wind velocity. Figure 1 depicts the signal quality for the Xband which operates at 9 HZ (=3.2cm). For higher

frequency the rate of deteriation as stated before is by the inverse square law. If lower frequencies are used the signal will improve by the square law but a tradeoff results in the resolution capabilities of the radar. The optimum band for both resolution and mimimum attenuation was the Xband.

Figure 2 is a graphical representation of the discussion in an earlier section. Since no definitive model of wind velocity versus backscatter has been established conclusively, this model was based on discussion by C.S. Cox [3].

Emission of Fluorescence Radiation from the Oil

Since oil has a fluorescence spectrum, two approaches may be used to record it. The first is to use an active UV device such as a laser to stimulate the fluorescence emission, and the second is to observe the natural fluorescence induced by the ambient sun and skylight. The latter approach is used with a passive sensor by measuring both the downwelling and upwelling radiation at a Fraunhofer line wavelength and a neighbouring wavelength. A strong fluorescence will be detected if the ratio of the upwelling on-Fraunhofer-line intensity/off-Fraunhofer-line intensity is greater than that for the downwelling signal.

5.0 OPERATIONAL PARAMETERS INFLUENCING THE SIGNAL

The choice of operational parameters such as look angle, altitude, time-of-day, etc. can significantly affect the results of a sortie and so their effects must be evaluated.

An IR sensor which operates in the thermal bands, say 8-14 μm, can work in both daylight and night. Solar heating of the oil surface occurs during the day, so that maximum contrast is expected with thick oil slicks in the daylight or early evening. Since oil has an emissivity different from water, even if the water and oil are at the same thermal temperature, some contrast between the two mediums is expected. Detection is not possible through fog, haze, rain, or clouds. Laboratory experiments have been conducted which show that petroleum products have strong IR bands at 3.3-3.5 μm, and 6.6-6.8 μm. Fish oils also show absorption here as well as 5.5-5.7 and 7.5-9.5 μm. Unfortunately the thermal background of the earth is too low at 3.3 μm and and

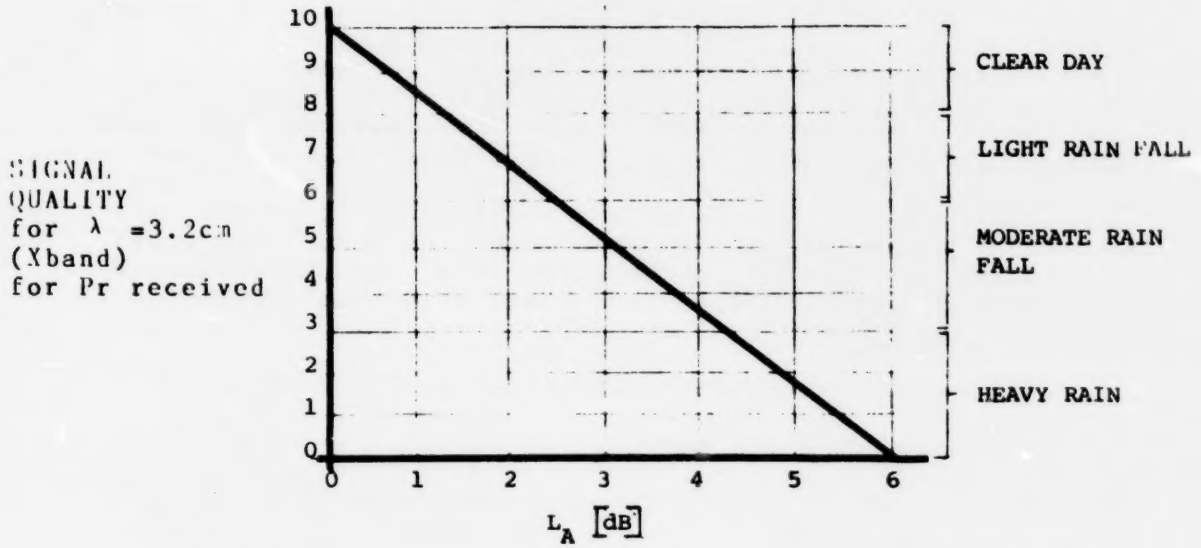

FIGURE 1 SIGNAL QUALITY VS ATTENUATION

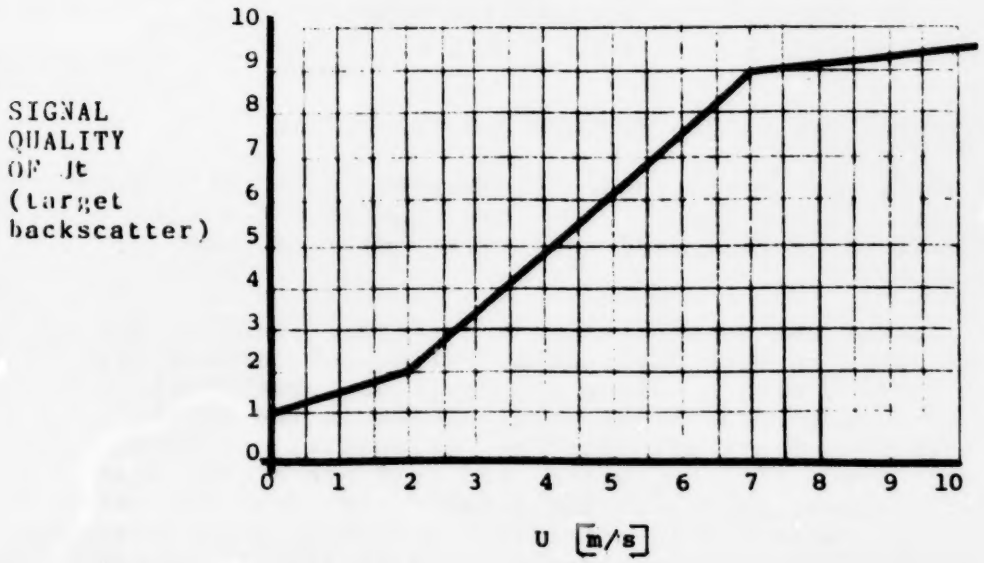

FIGURE 2 SIGNAL QUALITY VS WIND SPEED

the atmosphere is very opaque at 5.5 and 6.6 μm. This means that petroleum versus fish oil discrimination must be done using the 8-9.5 μm and 9.5-14 μm data.

The minimum contrast between water and oil is between .450-.500 μm, and the visible spectrum is defined from about .400-.650 μm, thus it seems that a visible light sensor is not as suitable for detecting oil on water.

Reception of ultraviolet (from .320-.380 μm) radiation depends on the reflected solar radiation, thus it is limited to daylight hours. In the UV, the contrast between oil and water depends on the oil type, slick thickness, solar illumnination, and on the water turbidity. Typically, very thin oils show the best contrast with water, and thicker portions of the slick are invisble.

5.1 Increased Surface Reflectance In The Near UV To Near IR

Overall, the oil layer tends to increase the surface reflectance of the water. However, the oil layer if sufficiently optically thick can reduce the volume reflected component, and thus lower the total reflectance.

A simple model of the components comprising the reflectance is

$$R_t = R_s + R_v + R_a$$

where

R_t - total reflectance

R_s - surface reflectance

R_v - volume reflectance

R_a - atmospheric reflectance

The oil is detected not by the actual value of reflectance but by contrast with the background. The contrast K is given by

$$K = \frac{R_o - R_b}{R_o + R_b}$$

where

R_o - measured reflectance of oil

R_b - measured reflecance of background

It is clear that the contrast will be maximized by maximizing the difference and minimizing the sum.

The most consistent results can be obtained by observing only the surface reflected light, this can be accomplished in a number of ways. By pointing the sensor toward the surface at Brewster's angle (approx. 53 degrees from the vertical for sea water), and observing the resultant beam through a linear polarizer, the surface reflection is passed and the volume component is reduced by up to 50%. Another method is to restrict the spectral range of the sensor to a region where the light absorption of water is high, say in the far-red and near IR.

The difference in the spectral variation of the surface signal of oil and water exhibits an important effect. The index of refraction of oil relative to water increases with decreasing wavelength, resulting in oil/water reflectance ratios which vary from 1.4 at 1.2 μm to 2.1 at .35 μm (Horvath, 1970).

The radiometric signal will be attenuated by the atmosphere and a noise term caused by scattering into the field of view of the sensor will be added to the signal. A simple model for this is

$$L_s = L_p + L_t * T_a$$

where

L_s - radiance at the sensor altitude

L_p - path radiance

L_t - target radiance

T_a - atmospheric transmittance

This may limit the altitude for the flight to reduce the atmospheric effect.

5.2 Change In Thermal Emissivity And/or Temperature

The real temperature and thermal emissivity of the oil/water will effect the apparent temperature seen by the sensor. The thermal emissivity of oil is typically less than that of water, therefore, oil at the same temperature as water will appear colder. In the temperature range 275-295 K a 1% reduction in the emissivity results in a 0.6 K drop in the apparent temperature. If the emissivity of oil is 2-5% less than that for water, then a 1-2.5 K contrast is expected (Buettner,1965) (Munday, 1971). Contrast due to real temperature differences will be highest at mid-afternoon on a clear day and contrast due to the difference in emissivity will be greatest on an overcast day with little wind.

5.3 Change In Radar Backscatter

The classical radar equation for microwave radars is

$$P_r = \frac{P_t G^2(\theta) \sigma_t \lambda^2}{(4\pi)^3 R^4}$$

where P_t = Peak power transmitted
$G(0)$ = One way antenna gain dependent on
σ_t = Radar target cross-section
λ = operating wavelength
R = Slant range to target
θ = incident angle from Nadir

since R = H sec θ
H = altitude of aircraft

then

$$P_r = \frac{P_t G(\theta)^2 \sigma_t \lambda^2}{(4\pi)^3 H^4 \sec^4 \theta}$$

The backscatter intensity is calculated from isolating Jt to the left side of the equation resulting in

$$J_t = \frac{P_r (4\pi)^3 H^4 \sec^4 \theta}{P_t G(\theta)^2 \lambda^2}$$

The calculated Jt is the backscatter intensity of the target area that was talked about previously. The signal Pr is the measured parameter which is used to calculate Jt while all other parameters are held constant.

Taking noise into consideration

$$J = \frac{P_r (4\pi)^3 H^4 \sec^4 \theta (KTB) NF}{P_t G(\theta)^2 \lambda^2}$$

where K = Boltzman's constant
T = absolute temperature of noise source at receiver of antenna.
B = Bandwidth of antenna
NF = Noise Figure

The parameters which are dependent on the characteristic of the radar system are Pt, B, NF, G(θ) and λ. Those parameters are basically constant or fixed and have little to do with variation of signal quality. On the other hand H and θ are variable and influence the signal quality of the calculated Jt, backscatter intensity.

Therefore, tradeoff results in obtaining optimum oil detection versus radar area coverage and resolution.

5.3.1 Altitude And Incident Angle Vs Radar Instantaneous FOV -

The two candidate radars that are looked at are the SCATTEROMETER and Side Looking Aperture Radar (SLAR). These two have been extensively used and developed for sea surface mapping and oil spill detection. In no way does the selection of these two radar system rule out any other existing radar systems but are here to be used as examples.

5.3.1.1 IFOV Calculation for SCATTEROMETER Type Radar

Variable Parameters

H = Altitude of Aircraft
θ = Antenna beamwidth fore aft/2
γ = Antenna beamwidth broadside

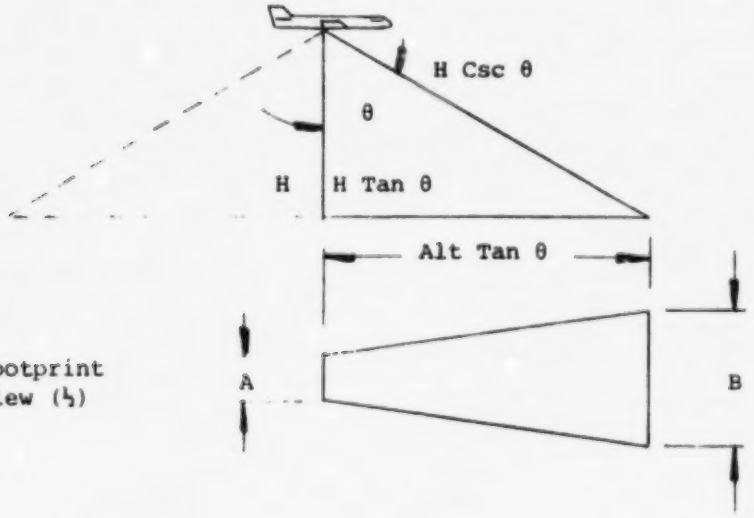

A = H x γ x π /180

B = (H x Csc(θ)) x γ x π /180

IFOV = 2 x area of trapezoid

= 2 x (A + B)/2 x Alt x Tan θ)

= γ x π /180 x H x H x
(1 + Sec(θ)**2) x Tan(θ)

.. IFOV = γ x π x H**2/180 x
(1 + Sec(θ)**2) x Tan(θ)

by first order trapezoidal approximation.

Effective IFOV Area for Detecting Oil Spills

For encompassing incident angles of 30deg to 55deg results in optimum oil detection.

.. IFOV(oil) = γ x π x H**2/180 x
(Sec(30)**2 + Sec(55)) x Tan(55-30)

= γ x π x H**2/180 x (2.04)

5.3.1.2 Calculation for IFOV for SLAR

Variable Parameters

γ = Beamwidth across track

β = Beamwidth along track

θ^1 = depression angle from horizontal adjusted by operator

H = Altitude of aircraft

SIDEVIEW

TOPVIEW

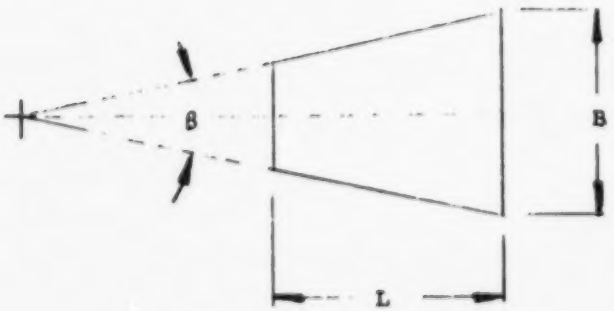

$IFOV = L \times B \times H$

$L = C \times \tau / (2 \times \cos(\theta^1))$

$B = ((\beta \times \pi)/180) \times H \times \csc(\theta^1)$

$\therefore IFOV = H \times C \times \tau / \cos(\theta^1) \times ((\beta \times \pi)/360) \times \csc(\theta^1)$

6.0 FALSE ALARMS

There exist a number of natural, and man-made occurances which an oilspill detection system would flag as real, but upon further investigation would be considered as false alarms. These are typically due to natural fish oil discharges from, say, a processing ship, or coastal processing facility, effluent seeps, anamolous signal variations due to changes in signal levels from cloud shadows etc. A summary of these phenomena anticipated to give false alarms, are summarized below.

Spectral Region	False Alarm Source
UV < 0.4 μm	- fish oil slicks - suspended solids - natural seeps - ice
Vis 0.4-0.65 μm	- fish oil slicks - suspended solids - shallow water - natural seeps - broken cloud cover
IR >.65 μm	- fish oil slicks - natural seeps
Thermal IR 3-14 μm	- fish oil slicks - natural seeps - ship waves - effluents - upwelling water currents
Microwave	- fish oil slicks - natural seeps - ship waves - effluents - upwelling water currents - ice

7.0 MINIMAL/MAXIMAL OIL DETECTABLE

7.1 Oilspils Sensor

For an oil layer of thickness D the evaporation rate in gms/sec is given by;

$$dm_{oil}/dt = p_{oil} A\, dD/dt$$

where p(oil) is the oil density and A is the area of the oilspill. If p(air) *A * h is the mass of air in a volume A * h above the spill then the fraction (by mass) escaping into the volume is simply;

$$dm_{oil}/dt/m_{air} = (p_{oil}/p_{air})(dD/dt)/h$$

The abundance measured by the Oilspills sensor is approximately;

$$F = 10^{6} m_{oil}/m_{air} h$$

so that

$$dF/dt = 10^{6} (p_{oil}/p_{air}) dD/dt$$

Assuming a measuremental integration time of 1 second for the sensor the minimum detectable abundance rate is

$$dF/dt \sim 400/\Delta T \qquad \text{ppm-m/sec}$$

Thus the minimum detectable evaporative rate;

$$dD/dt(min) = 400\times10^{-6} \times 1.2\times10^{-3}\ \text{gm/cm}\ /(.8\ \text{gm/cm}\ )/\Delta T$$

$$= .6/\Delta T \qquad \text{um/sec}$$

Clearly the oilspill layer must be of sufficient bulk and thickness to sustain such a rate for a significant period of time (.15 μm/sec for a 4 degree temperature contrast for example). In addition the temperature contrast which is a function of cloud cover, windspeed, and time of

day will effect a wide variation in the minimum detectable evaporative rate.

7.2 Radars

The maximum ratio of backscatter intensity from an area containing oil spill versus an area free from oil spills is dependent on incident angle. The proper selection of incident angle will yield an optimum in achieving an absolute maximum in the ratio. The larger the ratio the higher the probability in detecting oil spills from adjacent anomolies in sea surface structure. The optimum range in incident angle for detection of oil spills is within 30-55 deg. For the region 0-10 deg no possible distinction between ocean backscatter and oil slick backscatter was possible. For the region 10-30 deg and 55-60 deg a ratio of 5 to 7 dB is obtainable. For optimum incident angle range a ratio of 7-12 dB can be obtained. The following ranges were based on gathered flight test data of a SCATTEROMETER using 13.3 GHz frequency in VV polarization mode at Wallops Island on an actual oil spill [16]. The SCATTEROMETER incident angle is confined to + 60 deg from the planes vertical. For the SLAR the incident angle ranges from 0 to 90 deg , but no oil was present when flight tests were taken. From sea surface studies conducted in determining wind speed versus sea clutter the range of 30 deg-60 deg was shown to an optimum range for SLAR.

7.3 Lasers; Fluorosensor

Table 1 is a tabulation of minimum measurable thickness computations where as in reference 1 we have assumed that a S/N value of 3 is a minimal threshold for detecting signals with some information content. The choice of wavelengths (337 and 248 nm.) corresponds to the excitation wavelengths of a nitrogen and a more powerful excimer (KrF) laser. Results are given for a typical light oil (CO7) and a typical heavy oil (CO3) whose optical parameters are given in ref. [9]. As well we evaluate the effects of atmospheric transmission and altitude variations. Two states of atmospheric transmission are considered ; one corresponding to a horizontal visual range of 25 km. (ref. [11]) which is taken as typical for a clear day , and a second corresponding to a horizontal visual range of 5 km or a heavy haze. Three altitudes of 75, 300, and 750 meters

are denoted in the table by low, medium, and high respectively. The dashed entries indicate that no oil thickness will provide sufficient signal to obtain a signal-to-noise ratio of 3.

Table 1 - Minimum Thickness Calculations

Excitation wavelength	337 nm.	248 nm.
Absorption coefficients		
-light oil	.11	.76
-heavy oil	.6	2.7
Maximum conversion efficiencies [Nm**(-1)]		
-light oil	4E-4	4E-4
-heavy oil	1E-4	1E-4
Atmospheric transmission		
-23 km vis. range	.86	.67
-5 km vis. range	.48	.12

	Light oil			Heavy oil			Light oil			Hea
	low	med	high	low	med	high	low	med	high	low
Clear	.06	9.4	?	.04	.9	---	.0003	.005	.027	.0003
Hazy	.11	1.9	---	.08	2.2	---	.0015	.027	.16	.0017

d(min) [micromters]

8.0 OPERATIONAL ABILITY

8.1 Electro-optical Imaging Devices: Cameras

Television cameras may be configured to detect light over discrete band passes from UV thruough the IR spectrum to about 14 um.

Precipitation in the atmosphere will prevent a mission from being flown.

Visible and UV passive instruments are restricted to daylight flights, whereas IR imagers may be flown at night as well.

Infrared imagers are usable under clear day/night conditions but are unusable as the moisture content (fog, haze, clouds) of the atmosphere increases.

The following table 3 represents a summary of the operational ability of certain passive systems in various enviromental conditions. The scale is 0-10 with 10 being the highest rating.

Description of Ability	Thermal Infrared	LLLTV
Analysis System Commercially Available:	yes	yes
Oil Observation Ability for:		
Surveillance	8	7
Thickness	2	2
Specificity	0	0
Discern Oil Type:		
Heavy	0	0
Crude	0	0
Light Refined	0	0
Lighting Conditions:		
Day Clear	8	10
Day Overcast	8	6
Twilight	8	6
Night	8	0
Atmospheric Clarity:		
Clear	9	9
Haze	8	7
Precipition	0	0
Cloud	0	0
Fog	5	2
Wind/Sea State:		
Calm Base	10	10
Medium Base	7	7
High Base	3	3

Table 3 Operational Ability; Cameras

8.2 Electro-optical Imaging Devices: Scanners

Multispectral scanners may be configured to detect light over discrete band passes from UV thruough the IR spectrum to about 14 um.

Precipitation in the atmosphere will prevent a mission from being flown.

Visible and UV passive instruments are restricted to daylight flights, whereas IR scanners may be flown at night as well.

Infrared scanners are usable under clear day/night conditions but are unusable as the moisture content (fog, haze, clouds) of the atmosphere increases.

The following table 4 represents a summary of the operational ability of certain passive systems in various enviromental conditions. The scale is 0-10 with 10 being the highest rating.

Description of Ability	Thermal Infrared	Multi Spectral	Dual Channel UV and IR
Analysis System Commercially Available:	yes	yes	yes
Oil Observation Ability for:			
Surveillance	8	7	9
Thickness	2	2	5
Specificity	2	5	6
Discern Oil Type:			
Heavy	0	0	0
Crude	0	0	0
Light Refined	0	0	0
Lighting Conditions:			
Day Clear	8	10	9
Day Overcast	8	6	5
Twilight	8	3	5
Night	8	0	3
Atmospheric Clarity:			
Clear	10	10	10
Haze	9	7	8
Precipition	0	0	0
Cloud	0	0	0
Fog	6	2	3
Wind/Sea State:			
Calm Base	10	10	10
Medium Base	7	7	7
High Base	3	3	3

Table 4 Operational Ability: Scanners

8.3 Profiling Instruments

Multispectral profilers may be configured to detect light over discrete band passes from UV thruough the IR spectrum to about 14 um.

Precipitation in the atmosphere will prevent a mission from being flown.

Visible and UV passive instruments are restricted to daylight flights, whereas IR scanners may be flown at night as well.

Infrared profilers are usable under clear day/night conditions but are unusable as the moisture content (fog, haze, clouds) of the atmosphere increases.

The following table 5 represents a summary of the operational ability of certain passive systems in various enviromental conditions. The scale is 0-10 with 10 being the highest rating.

Description of Ability	Thermal Infrared	MPPH	OMA
Analysis System Commercially Available:	yes	no	no
Oil Observation Ability for:			
Surveillance	8	7	9
Thickness	2	2	5
Specificity	2	5	7
Discern Oil Type:			
Heavy	0	4	6
Crude	0	4	6
Light Refined	0	5	7
Lighting Conditions:			
Day Clear	7	10	9
Day Overcast	8	6	5
Twilight	8	2	2
Night	8	0	0
Atmospheric Clarity:			
Clear	10	10	10
Haze	9	7	7
Precipition	0	0	0
Cloud	0	0	0
Fog	3	2	2
Wind/Sea State:			
Calm Base	10	10	10
Medium Base	7	7	7
High Base	3	3	3

Table 5 Operational Ability; Profilers

8.4 Radars

Radars may be configured to detect microwave radiation in X,L or K bands.

Light to moderate precipitation in the atmosphere will not prevent a mission from being flown.

Radars may be flown at night as well.

Radars are usable under clear day/night conditions and are also usable as the moisture content (fog, haze, clouds) of the atmosphere increases.

Radars require that some capillary waves be present to detect the slick effect reduction in backscatter.

The following table 6 represents a summary of the operational ability of certain radars in various enviromental conditions. The scale is 0-10 with 10 being the highest rating.

Description of Ability	Scatterometer	SLAR
Analysis System Commercially Available:	no	yes
Oil Observation Ability for:		
Surveillance	8	9
Thickness	2	2
Specificity	2	2
Discern Oil Type:		
Heavy	0	0
Crude	0	0
Light Refined	0	0
Lighting Conditions:		
Day Clear	10	10
Day Overcast	10	10
Twilight	10	10
Night	10	10
Atmospheric Clearity:		
Clear	10	10
Haze	10	10
Precipition	6	6
Cloud	8	8
Fog	8	8
Wind/Sea State:		
Calm Base	0	0
Medium Base	10	10
High Base	7	7

Table 6 Operational Ability; Radars

8.5 Lasers

Laser fluorosensors cause UV oil fluorescence

Moderate precipitation in the atmosphere will prevent a mission from being flown.

Lasers may be flown at night or during day if they have the ability to subtract background radiance.

Lasers are usable under clear day/night conditions and are also usable with light fog or haze.

Laser positively identify oil type and thickness.

The following table 7 represents a summary of the operational ability of certain lasers in various enviromental conditions. The scale is 0-10 with 10 being the highest rating.

Description of Ability	Fluorosensor
Analysis System Commercially Available:	no
Oil Observation Ability for:	
Surveillance	2
Thickness	8
Specificity	10
Discern Oil Type:	
Heavy	10
Crude	10
Light Refined	10
Lighting Conditions:	
Day Clear	8
Day Overcast	8
Twilight	9
Night	10
Atmospheric Clearity:	
Clear	10
Haze	7
Precipition	4
Cloud	10
Fog	3
Wind/Sea State:	
Calm Base	10
Medium Base	9
High Base	8

Table 7 Operational Ability;

9.0 THE TEST PROTOCOL

The actual test protocol developed herein allows the comparison of any two sensors in any two classes, however it is often not meaningful to compare in an ad hoc way. Comparison within the general classes described should provide valid and useful information to the average user. The protocol is based on the optimal performance of each sensor to be compared and the expected degradation in the signal due to the prevailing atmospheric, oceanographic and operational conditions. For example Table 8 lists the performance parameters for two types of radar systems already mentioned (SCATTEROMETER & SLAR). The optimum for each performance parameter is dependent on the optimum magnitude obtainable for the backscatter variable Jt.

TABLE 8 Performance Parameters vs Radar System

	SCATTEROMETER	SLAR
Minimum Oil Detectable [m**2]	Beta.Vs x x H	1.5 x 1.2 (with optical or digital recorder)
Maximum Oil Detectable by Area Only[m**2]	IFOV(oil)	IFOV
Discrimination Between Thick & Thin Portion	NA *	NA
Daylight Dependency	None	None
Sea State Dependency	See Fig.2	See Fig.2
Optimum Incident Angle Range	30 deg - 55 deg	30 deg - 55 deg
Areal coverage [M**2/Hr]	Sw x Vs x 3600s/1Hr	
Vs:Aircraft ground Velocity	62-93 m/s	NA

* NA = Not applicable

Table 8 yields the geometric relations for each radar system to the performance parameters. Knowing the relationship between H and the radar equation, we can now introduce the invironmental and operational conditions into the performance parameter equation as shown in Table 8A for the SCATTEROMETER.

Table 1A: Test Protocol for Scatterometer Type Radar

Minimum Oil Detectable

$$BV_s \times \gamma \left[\frac{\sigma_T P_t G^2 (\theta) \lambda^2 L_A}{(KTB)NF \sec^4 \theta (4\pi)^3 P_r}\right]^{\frac{1}{4}} \qquad \left[M^2\right]$$

Maximum Oil Detectable

$$\frac{\gamma\pi}{180} (2.04) \left[\frac{\sigma_T P_t G^2(\theta) \lambda^2 L_A}{(KTB)NF \sec^4 \theta (4\pi)^3 P_r}\right]^{\frac{1}{4}} \qquad \left[M^2\right]$$

Aerial Coverage

$$V_s \times 3600 \times \gamma \left[\frac{\sigma_T P_t G^2 (\theta) \lambda^2 L_A}{(KTB)NF \sec^4 \theta (4\pi)^3 P_r}\right]^{\frac{1}{4}} \qquad \left[M^2/hr\right]$$

Lumping all constants together, the above performance parameter relation reduce to:

Minimum Oil Detectable

$$(\sigma_T \times L_A)^{\frac{1}{4}} \cdot K_1 \text{ where } K_1 = BV_s \frac{\times \gamma}{\sec \theta} \left[\frac{P_t G^2 (\theta) \lambda^2}{(KTB)NF (4\pi)^3 P_r}\right]^{\frac{1}{4}}$$

Maximum Oil Detectable

$$(\sigma_T \times L_A)^{\frac{1}{4}} \cdot K_2 \text{ where } K_2 = \frac{\gamma \pi}{180} \frac{(2.04)}{\sec^2 \theta} \left[\frac{P_t G^2 (\theta) \lambda^2}{(KTB)NF (4\pi)^3 P_r}\right]^{\frac{1}{4}}$$

Aerial Coverage

$$(\sigma_T \times L_A)^{\frac{1}{4}} \cdot K_3 \text{ where } K_3 = V_s \times 3600 \frac{\times \gamma}{\sec \theta} \left[\frac{P_t G^2 (\theta) \lambda^2}{(KTB)NF (4\pi)^3 P_r}\right]^{\frac{1}{4}}$$

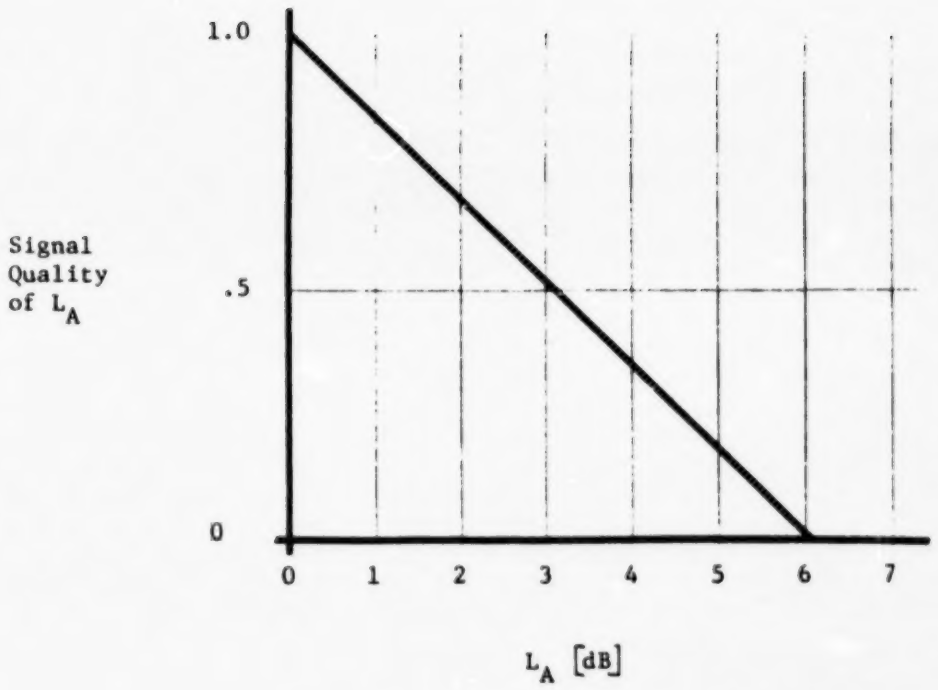

Figure 3: Signal Quality vs Attenuation

In Figure 2 the signal quality of Jt versus sea surface wind velocity is given as a range from 0-10. For simplicity the range is to be divided by ten to result in optimum conditions when the relationship of (Jt x La) = 1 and worst case when Jt x La = 0. the characteristic of the curve is the quadroot or squareroot of encompassing the Jt x La expression.

To determine the performance parameters for SLAR or any other radar type the same approach is to be used. Namely, replace the altitude parameter in the geometric expression in Table 8 by the classic radar equation whereby the altitude parameter is isolated on one side.

Table 1 is a geometric comparison but it can be use to determine actual parameters for the radar system under evaluation. Table 9 shows actual numbers for the SCATTEROMETER and SLAR radar system. With H = 5000 m and 0 = 45deg

	SCATTEROMETER	SLAR
Minimum Oil Detectable	6.33×10^{3} m^2	1.8 m^2
Maximum Oil Detectable	510×10^{3} m^2	86.4×10^{3} m^2
Sea State Dependency	U > 7 m/s	U > 7 m/s
Incident Angle	$30\text{-}55^{o}$	45^{o}
Areal coverage	87.7×10^{6} m^2 /hr	213×10^{6} m^2 /hr
Aircraft ground Velocity	93 m/s	93 m/s

TABLE 9 Performance Parameters for SCATTEROMETERS and SLAR for given Conditions

Results show SLAR to have advantages in resolution and areal coverage for conditions which yield an optimum for Jt for oil slick versus Jo for sea clutter.

10.0 DEMONSTRATION OF THE PROTOCOL

Using the SCATTEROMETER, as an example, we set the operating conditions at constant altitude and aircraft ground velocity. The environmental conditions are that of open sea with sea surface wind speed at greater than 7 m/s. Also, a rain cloud which is 500 metres in thickness and mass of 2.0 gm/m**3 causes an attenuation of 1.3 dB for

= 3.2 cm (f=9 GHz) and say, 3.7 dB for =2.2 cm (f=16.3GHz).

The value from Figure 2 for Jt = 10/10 = 1 and La from Figure 3 is 1/2. Therefore, the performance for the SCATTEROMETER for each of the performance parameters are listed in table 10:

	1 = 3.2 cm	1 = 2.25
Minimum Oil Detectable	$(1*.74)^{1/4} = .93$	$(1*.43)^{1/4} = .85$
Maximum Oil Detectable	$(1*.74)^{1/2} = .86$	$(1*.43)^{1/2} = .73$
Areal Coverage	$(1*.74)^{1/4} = .93$	$(1*.43)^{1/4} = .85$

Table 10 The comparison results

The above results indicate higher attenuation for smaller wavelengths. The assumption made between the two scatterometers is all other parameters are the same. Also the area required to detect oil has to be larger since the optimum value is now degraded.

11.0 SUMMARY

The protocol developed for the Scatterometer radar system can be applied to other radar systems by simply substituting the relationship of the altitude parameter(H) in the geometric relationship by the classic radar equation. Since geometries may differ between radar systems, a slightly different expression may be obtained every time.

By evaluating the performance parameters for each type of radar system one can then normalize using a reference or ideal radar system to get a relative quality factor among radar systems subjected to common environmental and operational conditions.

The general comparison serves as a rough protocol by which the sensor performances may be approximately compared. The detailed protocol requires detailed sensor descriptions and must be developed for each sensor that is to be included in the comparison.

12.0 REFERENCES

[1] J.F. Fanasia, T.M. Hard, and H.G. Ingra, "An investigation of Oil Fluorescence as a technique for Remote Sensing of Oil Spills", DOT transportation systems Centre, U.S. Coast Guard Report TSC-USCG-71-7(1971).

[2] R. Ho Varth, W.L. Morgan and S.R. Stewart, "Optical Remote Sensing of Oil Slicks: Signature Analysis and Systems Evaluation", Final Report, U.S. Coast Guard Project 124104.211 (1971).

[3] D.M. Rayner and A.G. Szabo, App. Opt. 17, 1624(1978)

[4] John P. Millard and John C. Averson, App. Optics, 11, 102 (1972)

[5] Takuzo SATO, Yoshihiro SUZUKI, Hiroshi KASHIWAGI, Motoi NANJO, The Transactions of the IECE of Japan, Vol E 61, 260 (1978).

[6] Michael Bristow, David Neilson, Donald Bundy and Robert Furtek, App. Opt. 20, 2889 (1981).

[7] American Society of Photogrammetry, Manual of Remote Sensing, Falls Church, Va., 1975.

[8] Lintz, J. and D.S. Simonett (eds), Remote Sensing of Environment, Addison-Wesley, Readings, Mass, 1976.

[9] Raynor, D. M., Thin Oil Film Detection Limits of Laser Fluorosensors, Report prepared for CCRS and EPS, EPS 4-EC-80-3, (1980).

[10] Raynor, D.M.,M. Lee, A.G. Szabo, Effect of Sea State on the Performance of Laser Fluorosensors, App. Opt., Vol. 17, P. 2730, (1970).

[11] Elterman, L., UV, Visible, and IR Attenuation for Altitudes to 50 km, 1968, Air Force Cambridge Research Laboratories, Report # AFCRL -68-0153.

[14] American Society of Photogrammetry "Manual of Remote Sensing", Vol II, Pg. 1556-1558, 1975

[15] American Society of Photogrammetry "Manual of Remote Sensing", Vol I, Pg. 208-211, 1955

[16] Jerlov, Neilson "Optical Aspects of Oceanography" 1974, Academic Press, Pages 51-60.

[17] O'Neill, R.A., et al. " The Arctic Marine Oilspill Program (AMOP) Remote Sensing Study ", Canada Centre for Remote Sensing, EPS 4-EC-83-3,

[18] Neville, R. A. Thomson, V., O'neil, R.A., Buja-Bijunas, L., Gray, L., Hawkins, B., Dagg, K., Remote Sensing of Oilspills", "Proceedings of the Arctic Marine Oil Spill Program Technical Seminar", Environmental Protection Service, Edmonton, Alberta, March 1979.

[19] O'Neil, R.A., "The Application O Presently Available Sensors for Airborne Oil Pollution Surveillance" Canada centre for Remote Sensing.

[20] -, "Remote Sensing Equipment for Chronic Oil Discharges", Bercha and Associates, EE-54, August 1984.

[21] Millard, J.P., Arveson, J.C., "Airborne Optical Detection of Oil on Water", Applied Optics, 11, p. 102-107, January 1972.

[22] Millard, J.P., Arveson, J.C., "Effects of Skylight Polarization, Coudiness, and View Angle on the Detection of Oil on Water", Proceedings of the Joint Conference on Sensing of Envirmental Pollutants, Palo Alto, Calif., November 1971.

[23] Rayner, D.M., Szabo, A.G., "A Laboratory Study of the Potential of Time-Resolved Laser Fluorosensors", CCRS Report # By-76-2(RC), 1976.

[24] Catoe, C.E., A Multispectral Look at Oil Pollution, Detection, Monitoring and Law Enforcement", CCRS # 1019756, 1979.

[25] Slater, P.N., "Remote Sensing; Optics and Optical Systems ". Addison-Wesley 1980, pp 427 - 30